Non-linear equivalent frame modelling:- Assessment of a two storey perforated unreinforced masonry wall

2012 NZSEE Conference

C.L. Knox

Holmes Consulting Group, Auckland, New Zealand.

J.M. Ingham

University of Auckland, Auckland, New Zealand.

ABSTRACT: The highly non-linear behaviour of unreinforced masonry walls makes linear static analysis methods inadequate and inaccurate and therefore for both academics and practicing engineers non-linear analysis of masonry buildings is preferable. Although accurate predictions of the structural response and cracking pattern can be generated by complex finite element (FE) meso models, the computational skill and high time cost often discounts this approach for everyday use. Alternatively, Equivalent Frame models are able to represent the essential characteristics of perforated wall response with minimal computational expense and can evaluate the key design parameters of ultimate strength, maximum displacement and failure mode.

The main features of the Equivalent Frame model used to represent the non-linear behaviour of unreinforced masonry perforated walls in SAP2000 are detailed. Closed-form solving of sectional equilibrium equations to evaluate the flexural strength of pier and spandrel components using a stress-strain relationship specific to New Zealand URM material behaviour which incorporates strain softening, is presented and used to define the coupled axial-moment hinge. Spandrel failure modes are developed and equations to capture the shear strength for each mode are presented. Finally a comparison between the modelled force-displacement response, and the experimentally obtained force-displacement response for full scale sub-structures and a two storey perforated wall previously experimentally tested is discussed.

1 INTRODUCTION

The large population of existing historically important unreinforced masonry buildings in New Zealand, and the continual exposure of the earthquake prone nature of unreinforced masonry as a construction material, have driven the need for accurate and efficient assessment techniques which will aid in the seismic retrofit process. The highly non-linear behaviour of perforated unreinforced masonry walls makes linear static analysis methods inadequate and inaccurate and therefore for both academics and practicing structural engineers non-linear analysis of unreinforced masonry buildings is preferable in order to fully describe their seismic capacity. In addition, the utilisation of performance-based earthquake engineering concepts involves the application of non-linear static procedures to evaluate the seismic performance of unreinforced masonry buildings. These procedures are based on a comparison between the seismic demand and the building capacity in terms of displacement. The building displacement capacity can be defined by a force-displacement curve ('pushover' curve) which describes the global inelastic response of the structure. This curve can be obtained by means of a non-linear static analysis, which involves subjecting the structure idealised using a modelling technique to a distribution of static lateral loads of increasing magnitude.

2 BACKGROUND

The idealisation of perforated unreinforced masonry walls can be achieved through different modelling approaches. Two main computationally based approaches can be identified in the literature: meso models, which employ the finite element (FE) method to describe a URM structure in detail by discretising the mortar and the brick units into multiple elements and adopting suitable constitutive laws, and macro models, which delineate the perforated wall into panels (spandrels and piers) in which the non-linear response is concentrated. Of this second type of modelling, Equivalent Frame models have been recognised as producing promising numerical results (Cattari and Lagomarsino 2008; Magenes *et al.* 2006; Pasticier *et al.* 2008). In the original non-linear models only the non-linear behaviour of piers was modelled, as there was little understanding of the performance of spandrels. In recent years the importance of the spandrel has been recognised and a number of research programmes have started to investigate and model the spandrel component (Beyer *et al.* 2010; Cattari and Lagomarsino 2008; Gattesco *et al.* 2010; Parisi *et al.* 2010). The findings from both a series of pier/spandrel substructure tests and the cyclic test on a two storey perforated wall highlighted the significance of the weak spandrel failure mode (Knox 2012) and therefore the need to allow for this type of response in the assessment procedure. In addition, from a survey of the New Zealand unreinforced masonry building stock it was found that shallow spandrels are present (Knox *et al.* 2009) and this occurrence was confirmed by photographic examples of spandrel damage that occurred during the February 2011 Christchurch earthquake, which proved that the phenomenon of spandrel damage and multi-storey pier response is not exclusively a laboratory induced mechanism. Hence the key to accurate modelling of perforated wall response is the correct representation of the spandrel strength and stiffness.

3 EQUIVALENT FRAME MODEL BASIC FORM

The non-linear Equivalent Frame models for each of the structures tested experimentally were defined using the software SAP2000 V14. The basic form of the non-linear model, including frame sectional properties, effective heights/lengths, rigid end off-sets, cracked section modification factors for Moment of Inertia and Elastic Modulus, and Material Property values, are discussed in Knox (2012) in detail.

The modelling reported herein characterised the non-linear behaviour of piers and spandrels by using a concentrated plasticity approach, with flexural plastic hinges located at each end of the effective pier and spandrel lengths, and shear plastic hinges located at mid points of the elements. The typical locations for pier and spandrel flexural and shear hinges are shown in Figure 1a for the two storey perforated wall and in Figure 1b for the substructures (PS1 shown as an example).

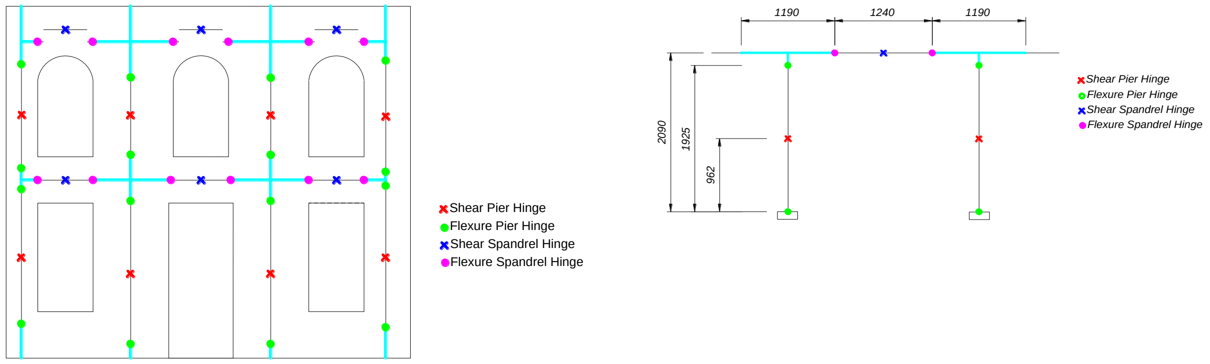

a) Hinge locations for two storey perforated wall *b) Hinge locations for pier/spandrel substructures (dimensions shown for PS1)*

Figure 1 Hinge locations for two storey perforated wall

4 PIER FAILURE MODE MODELLING

4.1 *Flexural failure*

The rocking capacity of piers is relatively well understood, with most techniques using an equivalent stress block technique as utilised in reinforced concrete design. An alternative approach is to calculate the moment-axial interaction curve from the closed-form solving of sectional equilibrium equations. This latter approach has multiple benefits: the effect of changing axial loads due to global rotation is captured, the equivalent stress block simplifications no longer need to be made, the interaction can be described in terms of strain ductility, and more realistic stress-strain models specific to unreinforced masonry can be adopted. From extensive masonry prism testing of both laboratory constructed prism samples using historical bricks, and from field prism samples, Lumantarna (2012) found that a stress-strain model with an initial parabolic variation, followed by post-peak softening and a linearly decreasing variation, and finally a constant stress tail was most representative of the true stress-strain relationship for New Zealand unreinforced masonry. Adopting the Lumantarna stress-strain relationship model, an expression for moment as a function of axial load and strain ductility is calculated assuming that for lime based historical mortar, mortar strength is generally less than 5 MPa and hence the strain at the ultimate limit state is equal to two times the yield strain and therefore the strain ductility is equal to 2. Solving for force and rotational equilibrium results in an expression for normalised moment capacity in terms of normalised axial load, and compression strain ductility is determined. Full numerical descriptions of the moment capacity equations are presented in Knox (2012).

The moment-rotation curve adopted for the pier flexural hinges is shown in Figure 2. An ultimate rotation of 0.02 (2%) was determined based on the upper bound limits found from experimental testing. Figure 3 shows the moment-axial force interaction curves for the proposed moment-axial failure domain based on the Lumantarna stress-strain profile and for a simplified elastic-perfectly-plastic (EPP) stress-strain relationship, as well as for the NZSEE (2006) pier moment capacity equation. The strength limit domains are shown as solid lines up to the point where the section changes from cracked to uncracked, which corresponds to a neutral axis depth equal to the height of the component. A comparison of the three strength limit domains shows that the moment capacity predictions vary significantly for normalised axial force in the range of [0.25,1], with the Lumantarna model predicting the most conservative moment capacities, and the EPP model predicting the least conservative. This reduction in moment capacity is mainly due to the presence of strength degradation in the Lumantarna model which reduces the compression force, which in turn reduces the moment capacity. It is hypothesised that as the Lumantarna strength domain is formed by adopting a realistic stress-strain profile, it can therefore be considered as the most accurate model. Under this assumption the NZSEE (2006) code-based formula results in a flexural strength overestimation for normalised axial forces greater than 0.25. To put this axial load interval in perspective, the ground floor piers of a five storey unreinforced masonry building with timber diaphragms will have a normalised axial force under dead loading of between approximately between 0.2 and 0.28, such that for normal loading conditions structures can be expected to be within the defined axial force bounds.

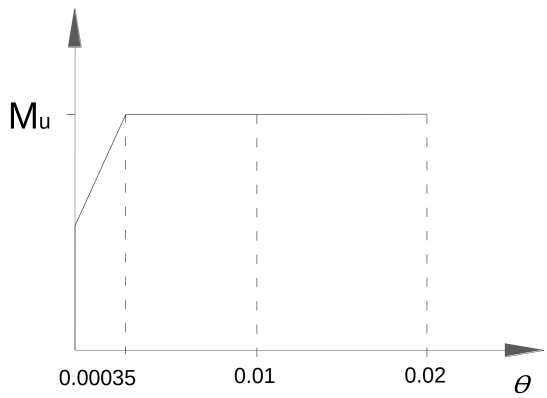

Figure 2 Moment-rotation backbone for piers

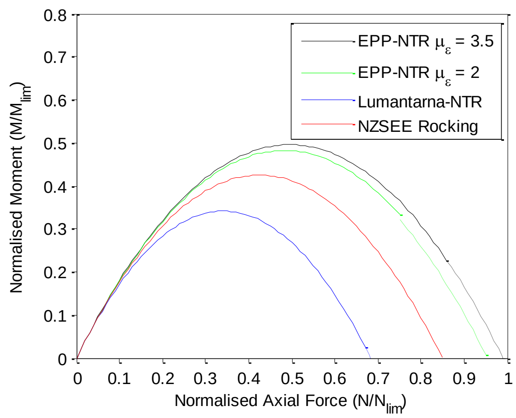

Figure 3 Moment-axial interaction curve for piers

4.2 *Shear Failure*

Current assessment guides define the nominal shear capacity as the minimum shear strength from sliding shear, diagonal cracking through the bricks, and diagonal stair stepped cracking following the mortar joints. For determining the nominal shear strength of piers within perforated walls, it is proposed that sliding shear is excluded as it has been shown to not be a primary failure mode for piers with aspect ratios equal to 1 or greater, but is extensively seen in very low aspect ratio walls, i.e.

aspect ratios greater than 0.5 (Ingham and Griffith 2011; Russell 2010). Sliding was evident during the pseudo-static testing of the two storey perforated wall (Knox 2012), however it occurred as a secondary failure mode, only ensuing after flexural response of the piers, at which stage the cohesion across the rocking surface is void. The nominal strength of a pier responding in a shear mode is therefore based solely on the shear strength associated with a diagonal tensile failure. Russell (2010) found that the diagonal tensile strength was accurately estimated by equation 1, and therefore this equation has been used to define the shear strength of piers.

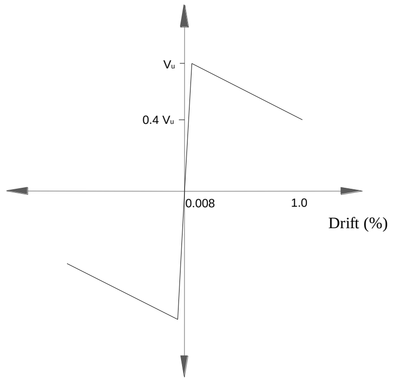

$$V_{dt} = \frac{0.9 b_p l_p f_{dt}}{\varsigma}\sqrt{1+\frac{\sigma_{avg}}{f_{dt}}} \qquad (1)$$

$$\textit{Slender piers where } {}^{h_p}/_{L_p} > 2.0 \quad \varsigma = 1.5$$

$$\textit{Stout piers where } {}^{h_p}/_{L_p} < 0.5 \quad \varsigma = 1.0$$

a) Force-dispalcement backbone curve for shear behaviour in piers

b) Governing equation for shear strength due to diagonal tension failure

Figure 4 Shear failure model for piers

5 SPANDREL FAILURE MODE MODELLING

5.1 *Spandrel Failure Modes*

The performance of perforated unreinforced masonry walls when subjected to lateral loading is significantly affected by the deformation and strength capacity of the spandrel panels. Lateral loads on multi-storey perforated walls result in low axial forces induced in the spandrel panels, coupled with high moment/shear demands, resulting in a force domain that is pointedly different from that of piers. In addition the interlocking nature of the bricks due to the bond pattern at the interface between the spandrel ends and the joints provides a coupling between the piers and spandrels. Three spandrel failure modes based on experimental results are shown in Figure 5, and are categorised as either shear (Mode B - diagonal cracking) or flexure modes (Mode A – Flexural cracking, and Mode C – Sliding).

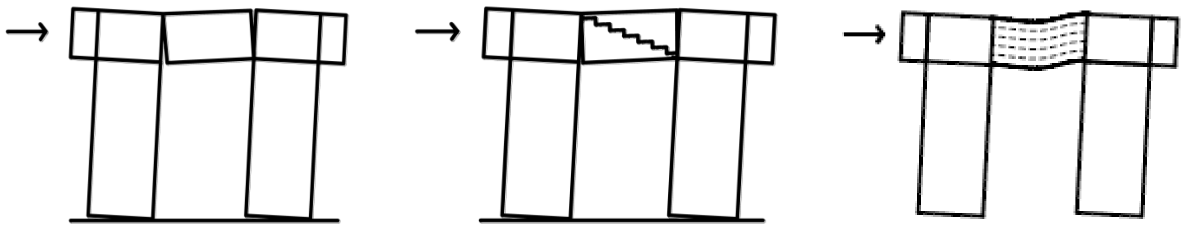

a) Mode A:Flexural cracking *b) Mode B: Diagonal cracking* *c) Mode C: Bending/ bed-joint sliding*

Figure 5 Spandrel deformation modes

5.2 *Flexural Failure*

A new proposal for calculating the moment-axial force strength limit domain for a spandrel is detailed. Cattari and Lagomarsino (2008) presented a strength criterion for the flexural behaviour of spandrels based on the model presented for piers, and applied to spandrels with the addition of an ‘equivalent’ tensile strength, based on the assumption of moment capacity being reached when the extreme compression fibre reaches the ultimate compression strain, i.e. when compression failure of the section occurs. It is proposed that this behaviour is not observed for spandrels, but instead the spandrel moment capacity is a function of the spandrel tensile strain in the extreme tensile fibres of the section. Rather than crushing of the masonry, sliding of the brick courses in the tension region of the section has been observed during the experimental programme reported in Knox (2012). It is therefore proposed that the equivalent tensile strength of the spandrel is based on the in-situ bed-joint shear strength.

A series of bed-joint shear strength tests were performed on the Aurora Tavern – a three storey unreinforced masonry building located in Auckland built in 1886, and on the Campbell Free Kindergarten – a two storey iconic unreinforced masonry building built in 1920. A generalised stress-strain model representative of the 'equivalent' tensile strength of spandrels based on the bed-joint shear strength tests is shown in Figure 6. The yield strain was determined from the average bilinear yield strain results. The ultimate strain was determined based on a maximum displacement of 10 mm. Shear strength can be determined from equation (2) which includes the Mann and Müller factor that accounts for the level of interlocking between bricks.

$$f'_t = \tau = \frac{\Delta x}{2\Delta y}(c + \mu N) \tag{2}$$

The moment-axial force domain for the proposed 'tension governed' model using the Lumantarna stress-strain model for compression behaviour is shown in Figure 7, in comparison to the failure domains determined using an EPP stress-strain model for compression, and for the case where no 'equivalent' tensile strength is allowed for. The addition of an 'equivalent' tensile strength is shown to make a marked difference in the moment capacity in the low axial load region which usually characterises the load on spandrels. Adopting the Lumantarna stress-strain profile for the constitutive equations in the sectional analysis results in a contracted limit strength domain compared to the EPP domain, which is due to the inclusion of strength degradation in the model.

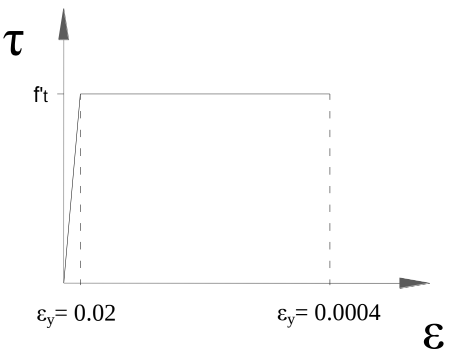

Figure 6 Generalised tension stress-strain model

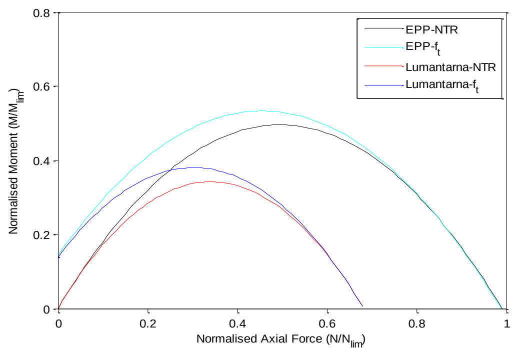

Figure 7 Moment-axial force limit domains for flexural failure in spandrels

5.3 *Shear Failure*

Shear failure in spandrels is characterised by the formation of diagonal cracking, with the cracks following the mortar joints when the ratio of brick compressive strength to mortar compressive strength is high. The characteristic 'X' crack pattern is consistent with the pattern observed in piers. Although the shear is acting perpendicular to the plane of the bed-joints within the spandrel, rather than parallel as is the case for piers, the bond pattern and structure of masonry means that the fundamental theory of diagonal stepped cracking is applicable to both piers and spandrels. Hence equation (1) is used to determine the shear capacity of spandrels, with a modification to the factor ς as detailed in equation (3) to allow for the different stress distributions within shallow and deep spandrels. To determine the nominal shear strength for a spandrel, the axial load acting on the spandrel at the ultimate limit state is required. The axial load is initially approximated by the maximum nominal shear strength of the adjacent pier. An iterative process can be followed to update the nominal shear strength of the spandrel by amending the value of axial load in the spandrel following analysis of

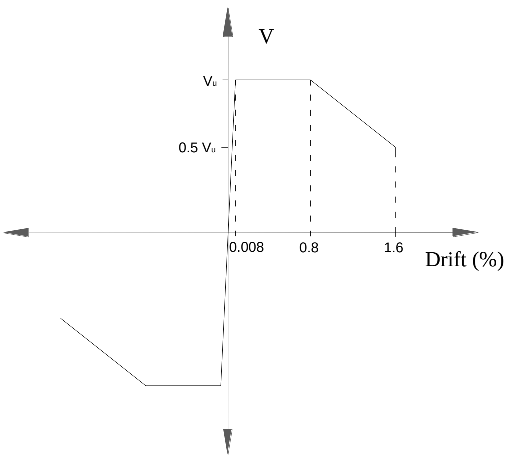

$$\frac{D_s}{L_s} > 1, \qquad \varsigma = \mathbf{1}$$

$$0.5 < \frac{D_s}{L_s} < 1, \qquad \varsigma = \frac{D_s}{L_s} \tag{3}$$

$$\frac{D_s}{L_s} < 0.5, \qquad \varsigma = \mathbf{1.5}$$

a) Force-displacement backbone curve for shear behaviour in spandrels

b) Governing equation for shear strength due to diagonal tension failure

Figure 8 Shear failure model for spandrels

the model. Figure 8a shows the force-displacement curve adopted for shear failure in spandrels. The perfectly plastic branch of the curve is extended to a drift of 0.8% based on the experimental results reported in Knox (2012), followed by a degrading stiffness branch.

6 EQUIVALENT FRAME ANALYSIS RESULTS

The equivalent frame model described herein has been validated by comparing the model push-over curve and deformed shape with the experimental results from the six substructure tests and from the two storey perforated wall test reported in Knox (2012). The experimental force-displacement backbone and the pushover curve are shown in Figure 9(a-c) for substructures PS1, PS2 and PS3 respectively, with the predicted strength according to the NZSEE (2006) guidelines overlaid for comparison. The force-displacement plots illustrate the significant over-estimation of lateral strength obtained as a result of assuming the spandrel to be rigid. Good agreement between the experimental backbone curve and the pushover curve from the EF model is shown, highlighting the importance of the spandrel element in the global assessment of a perforated wall.

The Equivalent Frame model for the two storey wall predicted a weak spandrel mechanism, with the deformed shape showing that the spandrel flexural hinges in the central spandrel were activated, and that the top spandrels failed in a mixed flexural-shear response as shown in Figure 9d. In addition, the model correctly predicted the individual rocking of the Pier A ground and first floor piers, and the double-storey height pier rocking in pier C, although a flexural hinge occurred at the top of ground floor Pier B which was not consistent with the experimental observations. The proposed constitutive equations and idealised behaviour curves are further validated by the good agreement of the model pushover curve with the experimental backbone curve, with the Equivalent Frame model correctly predicting the maximum shear force, the overall response, and the ultimate displacement within practical limits as shown in Figure 9e.

7 DISCUSSION

As is the case with most computational modelling tools, the level of accuracy that may be obtained is limited by the accuracy of the information that the model draws on. Within the Equivalent Frame model with lumped non-linearity there are a number of sources of uncertainty that will influence the accuracy of the model. Where the material properties of the masonry used in the construction of the test specimens were expressly measured, it has been shown that the elastic stiffness and non-linear behaviour of the wall can be accurately modelled using the Equivalent Frame model. For assessment of buildings by practicing engineers, where a comprehensive material testing programme cannot be

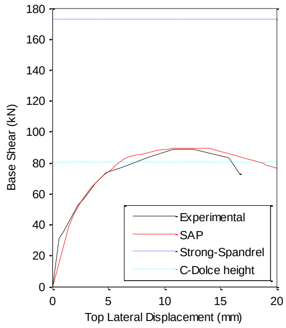

a) Force-displacement backbone for PS1

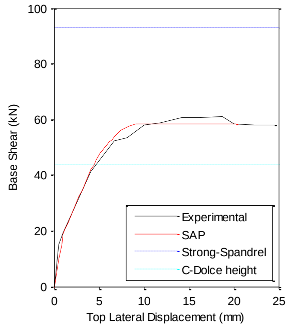

b) Force-displacement backbone for PS2

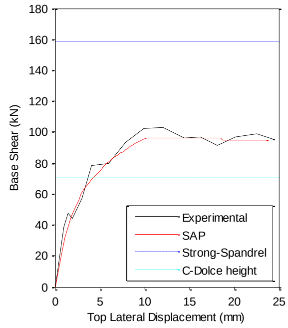

c) Force-displacement backbone for PS3

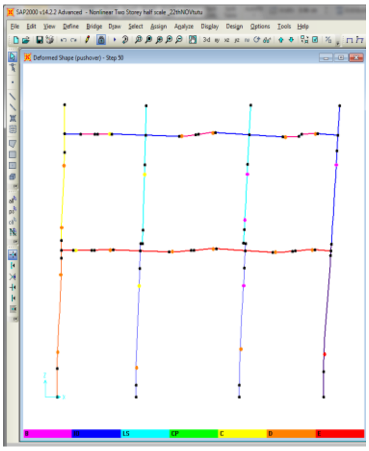

d) Deformed shape for two storey perforated wall

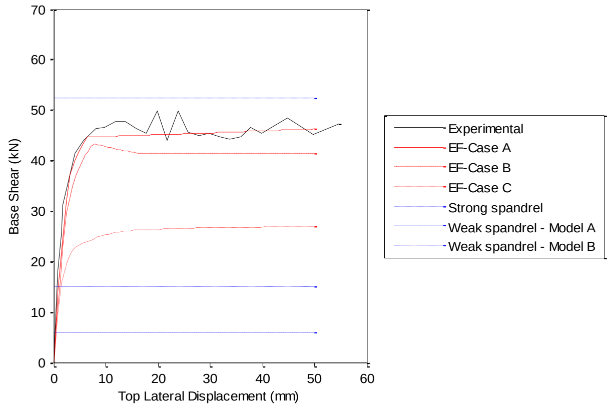

e) Force-displacement backbone for two storey perforated wall

Figure 9 Equivalent Frame model results

undertaken for each building, the material properties are often taken from an assessment guide which provides a range of values depending on the quality of the materials. Lumantarna (2012) has shown that the range of probable values for each material property is large, and importantly this variability can result in a change of critical failure mode. In addition, unreinforced masonry is a historical construction material laid by hand, and it is therefore not surprising that often extensive variability in material quality and properties is common within one building. This uncertainty and variability of material properties not only affects the non-linear behaviour but also the elastic stiffness of the perforated wall, as the elastic stiffness is a direct function of the Young's Modulus and Shear Modulus of masonry. A softening or hardening of the elastic stiffness will also affect the maximum lateral strength and drift at yield.

The proposed method for determining the 'equivalent' tensile strength for the spandrel element for use in calculating the moment-axial force interaction curve was shown to provide good agreement with the experimental results, for both failure mode and maximum lateral strength. Noteworthy is that the model is sensitive to changes in the 'equivalent' tensile strength, with higher values causing strengthening of the spandrel and over estimating the global lateral strength, and low values creating a weak spandrel model.

The main disadvantage of the proposed method for assembling the non-linear Equivalent Frame method is the uncertainty of the axial load on the spandrel at the ultimate limit state, which in turn defines the spandrel diagonal shear capacity. In order to overcome this, the development of an interacting axial-shear hinge in SAP2000, or any equivalent finite element programme that is accessible to practising engineers, is required.

8 CONCLUSIONS

The non-linear behaviour of the perforated wall was idealised using hinges and non-linear links positioned at the centre and ends of the pier and spandrel frame elements to represent shear and flexural failure respectively. Pier and spandrel flexural behaviour was modelled using an interacting moment-axial hinge based on an interaction curve generated from closed-form solving of the sectional equilibrium equations and a specialised non-linear stress-strain behaviour model developed by Lumantarna (2012) for New Zealand unreinforced masonry. The equation for diagonal shear failure proposed in NZSEE (2011) was adopted for shear failure in piers, and with a modification to the aspect ratio factor, was also adopted for shear failure in spandrels. Additionally, by modelling the flexural behaviour of the piers and spandrels with an interacting moment-axial force hinge, the effects of overturning and redistribution of axial loads were accounted for.

Non-linear static modelling employing the Equivalent Frame method was conducted using the widely available software SAP 2000. The pushover curves were found to provide good agreement with the experimental backbone curves obtained from the substructure testing programme and the two storey perforated wall test. In addition, the analysis is highly time efficient, taking less than two minutes to run, although construction of the model requires some technical skill and time input. The advantage of accuracy outweighs the simplicity of the current simplified methods, whilst still being superior in efficiency and time over finite element modelling.

9 REFERENCES

Beyer, K., A. Abo El Ezz and A. Dazio (2010) 'Experimental investigation of the cyclic behaviour of unreinforced masonry spandrels', Proceedings of the 9th US National and 10th Canadian Conference on Earthquake Engineering, Toronto, Ontario, Canada.

Cattari, S. and S. Lagomarsino (2008) 'A Strength criterion for the flexural behaviour of spandrels in unreinforced masonry walls', The 14th World Conference on Earthquake Engineering, Beijing, China.

Gattesco, N., L. Macorini, I. Clemente and S. Noe (2010) 'Shear resistance of spandrels in brick-masonry buildings', 8th International Masonry Conference, Dresden, Germany.

Ingham, J.M. and M.C. Griffith (2011) 'Performance of New Zealand's masonry buildings during the 2010 Darfield (Christchurch, NZ) earthquake', *Australian Journal of Structural Engineering,* **11**(3),321-339.

Knox, C., Q.T. Ma and J.M. Ingham (2009) 'Assessing the rocking response of unreinforced masonry frames in historical New Zealand Structures', Protection of Historical Buildings, First International Conference, Rome.

Knox, C.L. (2012) 'Assessment of Perforated Unreinforced Masonry Walls Responding In-Plane', Department of Civil and Environmental Engineering, University of Auckland, PhD Thesis, New Zealand.

Lumantarna, R. (2012) 'Material Characterisation of New Zealand Unreinforced Masonry Buildings', University of Auckland, PhD Thesis, Auckland.

Magenes, G., M. Remino, C. Manzini, P. Morandi and D. Bolognini (2006) 'SAM II Software for the simplified analysis of masonry buildings', University of Pavia and EUCENTRE.

NZSEE (2006) 'Assessment and Improvement of the Structural Performance of Buildings and Earthquakes - Recommendations of a NZSEE Study Group on Earthquake Risk Buildings' New Zealand Society for Earthquake Engineering, Wellington.

Parisi, F., N. Augenti, A. Balsamo, A. Prota and G. Manfredi (2010) 'Lateral load tests on a masonry system with and without external reinforcement', 14th European Conference on Earthquake Engineering, Ohrid, 30th August - 3rd September.

Pasticier, L., C. Amadio and M. Fragiacomo (2008) 'Non-linear seismic analysis and vulnerability evaluation of a masonry building by means of the SAP2000 V.10 code', *Earthquake Engineering and Structural Dynamics,* **37**(3),467-485.

Russell, A.P. (2010) 'Characterisation and Seismic Assessment of Unreinforced Masonry Buildings', University of Auckland, PhD Thesis, Auckland.